

# A New Approach on Skull Stripping of Brain MRI based on Saliency Detection using Dictionary Learning and Sparse Coding

## Nuevo Enfoque en la Extracción del Cráneo en MRI Cerebrales basado en la Detección de Prominencias Mediante el Aprendizaje de Diccionarios y la Codificación Dispersa

Nallig Leal<sup>1</sup> and Eduardo Zurek<sup>2</sup>

<sup>1</sup> Msc. Profesor de Tiempo Completo, Universidad Autónoma del Caribe, Grupo de Investigación SINT-UAC, Barranquilla. E-mail: nleal@uac.edu.co

<sup>2</sup> Ph.D. Profesor de Tiempo Completo, Universidad del Norte, Grupo de Investigación en Robótica y Sistemas Inteligentes, Barranquilla. E-mail: ezurek@uninorte.edu.co

**Cite this article as:** N. E. Leal Narváz, E. E. Zurek Varela "A New Approach on Skull Stripping of Brain MRI based on Saliency Detection using Dictionary Learning and Sparse Coding", *Prospectiva*, Vol 17, N° 2, 25-32, 2019

**Recibido: 17/06/2019 / Aceptado: 05/07/2019**

<http://dx.doi.org/10.15665/rp.v17i2.2050>

### ABSTRACT

*In brain magnetic resonance images (brain MRI) analysis, for diagnosing certain brain conditions, it is necessary to quantify the brain tissue, which implies to separate the brain from extracranial or non-brain tissues through a process of isolation known as skull stripping. This is a non-trivial task since different types of tissues may have the same gray level, and during the separation process, some brain tissues could be removed. This paper presents a new solution approach for the skull stripping problem, based on saliency detection using dictionary learning and sparse coding, which can operate over T1 and T2 weighted axial brain MRI. Our method first subdivides the axial MRI into full overlapped patches and runs a dictionary learning over them for obtaining its sparse representation. Then, by analyzing the sparse coding matrix, we compute how many patches a dictionary atom affects to classify them as frequent or rare. Then, we calculate the saliency map of the axial MRI according to the composition of the image patches, i.e. an image patch is considered salient if it is mainly composed of frequent atoms, an atom is frequent whether it affects many patches. The non-salient pixels, corresponding to non-brain tissues, are eliminated from the MRI. Numerical results validate our method.*

**Keywords:** Skull stripping, MRI, Saliency detection, Dictionary learning, Sparse coding.

### RESUMEN

*En el análisis de Imágenes de Resonancia Magnética cerebral (IRM cerebral), para diagnosticar ciertas afecciones cerebrales, es necesario cuantificar solo el tejido cerebral, por lo que éste se debe aislar del tejido no cerebral. Esta es una tarea no trivial que involucra la separación de diferentes tipos de tejidos que pueden tener el mismo nivel de gris. Este artículo presenta un nuevo enfoque para solucionar el problema de la extracción del cráneo, basado en la detección de prominencias mediante el aprendizaje de diccionarios y codificación dispersa, que puede operar en IRM axiales potenciadas en T1 y T2. Nuestro método subdivide la IRM axial en parches superpuestos y ejecuta aprendizaje de diccionario para obtener su representación dispersa. Luego, analizamos la matriz de codificación dispersa y calculamos cuántos parches de imagen afecta un átomo del diccionario, para clasificarlo como frecuente o raro. Luego, calculamos el mapa de prominencia de la IRM axial según la composición de los parches de la imagen. Un parche de imagen se considera prominente si está compuesto principalmente de átomos frecuentes, un átomo es frecuente si afecta muchos parches. Los píxeles no prominentes, correspondientes a los tejidos no cerebrales, se eliminan de la IRM. Resultados numéricos validan nuestro método.*

**Palabras Claves:** IRM, Extracción del cráneo, Detección de prominencias, Aprendizaje de diccionarios, Codificación dispersa.

## 1. INTRODUCTION

One of the most important techniques that can provide images about the interior of the human body is the Magnetic Resonance Imaging (MRI). This is a non-invasive radiological technique, which allows obtaining internal information from the human body through detailed and high contrast images for diagnostic purposes in the medical field. MRI bases its operation on the phenomenon of magnetic resonance, avoiding the use of ionizing radiation, as in the case of Computerized Tomography (CT).

Radiologists can make qualitative analyzes of an MRI; however, this can be subjective, since it depends on the knowledge and experience the radiologist has. In cases where quantitative analysis is required, automatic segmentation is necessary. The quantitative analysis, like morphometric analysis, helps in the diagnosis of different pathologies and the evaluation of the response to a given treatment. However, the automatic segmentation of the tissues present in an MRI is not a trivial task, since it must be considered that, for example, different types of tissues can have similar gray levels, there are no absolute values in the units of intensity, the inhomogeneity and the inherent noise associated with an MRI [1].

Quantitative morphometric studies based on brain MRI, normally require separating the brain from extracranial or non-brain tissues through a process of isolation known as skull stripping [2]. Studies in discovery biomarkers for dementias like Alzheimer's Disease [3], [4] and Schizophrenia [5] [6], early detection of Huntington's Disease [7], [8], and tissue classification [9], among many others, process skull stripped brain MRI. Skull stripping of brain MRI is a challenging task that continue being an active research problem, which has different solution approaches [10] [11] [12] [13] [14], all of them have their advantages and disadvantages. In this paper, we present a simple solution from a new approach based on saliency detection using dictionary learning and sparse coding, which operates indistinctly over T1 and T2 weighted axial brain MRI.

Our method first runs dictionary learning over the MRI patches for obtaining its sparse representation. Then, by analyzing the sparse coding matrix, we compute the frequency of appearance of the atoms in the image patches. Then, we calculate the saliency map of the MRI according to the composition of the image patches, i.e. an image patch is considered salient if it is mainly composed of frequent atoms, an atom rare whether it affects few patches. The salient pixels that correspond to non-brain tissues are eliminated from the MRI.

This paper is organized as follows. Section 2 presents related work. Sections 3 and 4 present the fundamentals of

Visual saliency and Dictionary Learning and Sparse Coding, respectively. Section 5 presents the proposed method for skull stripping on brain MRI. Section 6 presents the results and discussion. Finally, in Section 7 the conclusions of this work are presented.

## 2. RELATED WORK

The goal of skull stripping is to isolate the brain from extracranial or non-brain tissues, which is a challenging task that has received several solution approaches. Since the morphological approach proposed by Brummer et. al. [15] in 1993, many others have been proposed. More recently, in 2015, Roy and Maji [16] presented a hybrid approach based on pixel intensity and morphological operations for skull stripping on T1 weighted MRI. The method consists of a sequence of steps that apply typical spatial techniques of digital image processing, like median filter and thresholding, in addition to morphological operations such as opening and closing. In this approach, parameters like thresholds and structuring elements of the morphological filters, require previous statistical studies to estimate the suitable values for such parameters since, like was mentioned before, different types of tissues may have the same intensity levels, there are no absolute values in the units of intensity, the inhomogeneity and the inherent noise associated with the MRI [1], factors that may vary from one MRI to another one.

A different approach for skull stripping from deep learning was proposed in 2016 by Kleesiek et. al. [17], which can operate over non-enhanced and contrast-enhanced T1, T2 and FLAIR MRI. They proposed a 3D convolutional deep learning architecture for processing the MRI. The proposed consist of a convolutional neural network of seven hidden layers and one output-layer, where each layer implements a spatial 3D convolution filter that performs a point-wise non-linear transformation. Each layer represents a specific number of filters with a fixed size pre-established. The neural network can deal with image artifacts like tumors.

This method reports good results, even outperform some state-of-the-art methods, for certain public data sets. However, it is necessary to select a training set representative of the global data to achieve good training of the network for obtaining such good results. The training process takes around fifteen hours and it is necessary to run it every time the data set is changed since this is a supervised process.

An approach from fuzzy logic was proposed by Roy and Maji in 2018 [10]. Based on the rough-fuzzy connectedness of a voxel, term that refers to the degree of membership of the voxel respect to the brain region as long with the degree of adjacency to it, this method can discern whether a given voxel belongs to brain tissue even between two different types of

regions where the boundary is affected by the blurring effect. The method can deal with both healthy and diseased brain MR images. Due to the dependency of the rough-fuzzy connectedness of a voxel on the gray level, this method only can deal with T1 weighted brain MR.

We present a novel approach, simple and robust, from visual saliency, using dictionary learning and sparse coding, which is independent of the contrast, which does not require previous training either the manual configuration of parameters, since it is automatically adjusted according to the conditions of the image. Besides, our method can deal with both T1 and T2 weighted brain MRI.

### 3. VISUAL SALIENCY

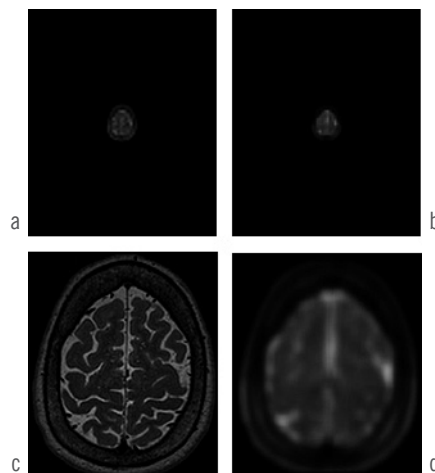
The human brain and the human vision system, in front of a given scene, focus on regions with more information. Many studies in the field of psychology, neuropsychology and cognitive neurosciences, have detailed how the extraction of such information is carried out, even proposing models of the functioning of visual attention. From these models, computer scientists have proposed computational variants [18] [19] [20] [21], which imitate human visual attention. This field of research is known as saliency detection on images.

Detection of saliency is a key component that is used as an input to solve much more complex problems such as image segmentation, object extraction from the background, and compression of images, among others [19]. In this work, visual saliency is used for detecting brain tissue.

There exist two main classification models about how the brain computes visual saliency [22]. The Top-Down model, based on supervised learning, reaches high performance especially when deep learning techniques are used. The Bottom-Up model, the most used in solution approaches in computer sciences [23], suggests that the brain focuses on low-level vision features [22] like rare patterns, among others. From this, it can be inferred that the term “focuses”, refers to the differentiation between rare patterns and common patterns, which is equivalent to a classification. Then, it is possible to classify image regions by detecting rare or common patterns on them. Our method for skull stripping on brain MRI is based on the Bottom-Up, because it is supported on identifying rare patterns, or regions with a high level of irregularity (regions with more information) for detecting salient regions.

The regions with more information (salient regions) of an axial brain MRI are related to patterns where sinuous brain structures are present. Figure 1a shows an image where the common pattern is the black background, and the rare pattern is the small brain in the center.

Figure 1. Salient region due to rare patterns  
Figura 1. Región prominente debido a patrones extraños



In Figure 1a, the attention is focused on the small brain in the center of the image, due to the rarity of this region respect to the rest of the image, therefore this is a salient region. However, if zoom in of such a region is made, the rare patterns change, and also the salient regions. Figures 1c and 1d show this new situation. Now, in Figure 1c, the more irregular region (rare patterns) is the brain tissue (highlighted region in figure 1d); however, some cranial and fatty tissues, (outer rings), are also salient in a lesser extent, therefore would be necessary to increase the saliency of the inner regions and decrease the saliency of outer ones, in order to heighten the difference between the saliency level of these types of tissue. Based on this, our method will detect non-brain tissue to carry out the skull stripping process. The rare patterns will be detected using the sparse representation of the image regions. This will be addressed in section 5.

### 4. DICTIONARY LEARNING AND SPARSE CODING

Sparse representations in neuroimaging are useful for a better understanding of the brain functioning, besides just learning predictive models of mental states from imaging data [24]. It has been used in conjunction with SVM for the classification of Alzheimer’s disease [25], and jointed with Dimensionality Reduction [5] for estimating Schizophrenia biomarkers from fMRI. In both cases, the accuracy of the classification of cases and controls was improved.

Dictionary Learning is a form of sparse representations which is aimed to find, from a set  $\mathbf{Y}$  of data, also called signals, a dictionary  $\mathbf{D}$  so that  $\mathbf{Y}$  can be sparsely approximated from  $\mathbf{D}$ , i.e.  $\mathbf{Y} \approx \mathbf{D}\alpha$ . Where  $\alpha$  is a sparse matrix known as the sparse coding matrix or the sparse representation of  $\mathbf{Y}$ . On the other hand, the purpose of sparse coding is to approximate a set of feature input vectors as a linear combination

of basis vectors, called atoms, which are selected from the dictionary learned from the data themselves.

In a formal way, let  $\mathbf{Y}$  be a set of  $p$   $n$ -dimensional signals  $\mathbf{Y}=\{y_1, y_2, \dots, y_p\}$ , the dictionary learning and the sparse coding aims to find a dictionary  $\mathbf{D} = \{d_1, d_2, \dots, d_N\}$  and a sparse matrix  $\alpha$  such that  $\mathbf{Y}$  can be approximated by a linear combination of the basis vectors  $d_i$  (atoms). This is,  $\mathbf{Y} \approx \mathbf{D}\alpha$ , where most of the coefficients  $\alpha_{i,j}$  are zeros or close to zero [26]. We have that, the dictionary learning and the sparse coding problem can typically be formulated as an optimization problem, how indicates Equation 1.

The KSVD algorithm proposed in [27] allows obtaining the optimal values of  $\mathbf{D}$  and  $\alpha$  in Equation 1. By analyzing the sparse representation of the set of signals in  $\mathbf{Y}$ , it can be detected some features about them. e.g. it is possible to know if a given signal represents or belongs to a rare pattern on an image and therefore to know whether a region is salient or not. This will be addressed in the next section.

## 5. PROPOSED METHOD

Our solution approach for the problem of skull stripping on brain MRI consists of three steps. However, an initial preprocessing is carried out for obtaining the more suitable starting point. These stages are presented below.

### 5.1 Preprocessing stage

Depending on the depth of the slice, an axial brain MRI may present different patterns, i.e. in a slice near the top of the volume, common patterns could be empty, flatten or homogeneous regions, like shows Figure 2a. There may be no brain tissue in these slices. In a middle slice, the sinuous brain structures are the common pattern, like shows Figure 2b. In a deeper slice, the patterns are more varied (see Figure 2c) as a result, the salient regions could correspond to non-brain tissue, and no be segmented. Therefore, the starting point of our method is a middle slice.

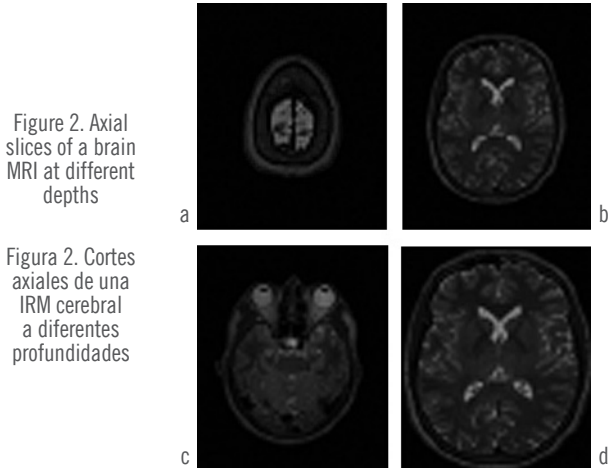


Figure 2. Axial slices of a brain MRI at different depths

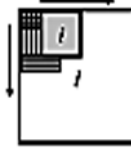
Figura 2. Cortes axiales de una IRM cerebral a diferentes profundidades

Before processing the slice looking for salient regions, it is necessary to crop the image to highlight the salient regions, like it is illustrated in Figure 2d. This is because without cropping the image, the rare pattern could be the whole brain including the skull, which would make salient non-brain tissues that we want to remove like was shown in Section 4 (see Figure 1a and Figure 1b).

### 5.2 Dictionary Learning

Once we have the initial slice  $I$ , it is divided into full overlapped  $\sqrt{n} \times \sqrt{n}$  patches, i.e. we shift a sliding patch each pixel in both horizontal and vertical direction, as illustrates Figure 3.

Figure 1. Salient region due to rare patterns  
Figura 1. Región prominente debido a patrones extraños



Then each patch  $i$  is converted into a vector (signal)  $y_i \in \mathbb{R}^{n \times 1}$ , with  $n = 64$  in our tests. Then we conform the signals matrix  $\mathbf{Y}=\{y_1, y_2, \dots, y_p\} \in \mathbb{R}^{n \times p}$  where  $P$  is the number of patches. A sparse coding matrix  $\alpha \in \mathbb{R}^{K \times p}$  and a dictionary  $\mathbf{D} \in \mathbb{R}^{n \times K}$  according to dictionary learning and sparse coding theory are defined.  $K$  is the number of atoms of the dictionary (in our tests  $K$  was set to 30 for processing images of  $168 \times 168$  pixels). Solving Equation 1 using the KSVD algorithm proposed in [27] [28] the optimized version of  $\alpha$  and  $\mathbf{D}$  are obtained. Now,  $\mathbf{Y}$  can be reconstructed as  $\mathbf{Y} = \mathbf{D}\alpha$ . As a result, we have the sparse representation of  $\mathbf{Y}$  in  $\mathbf{D}$ , and we can estimate the rarity of a signal  $y_i$  by analyzing  $\alpha_{i,j}$ .

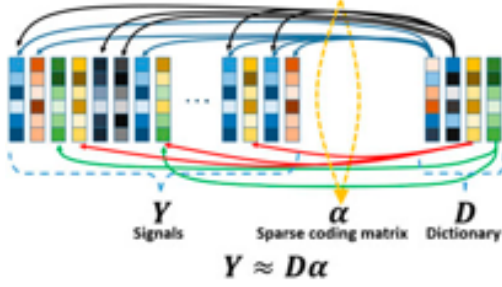
### 5.3 Frequency estimation of the atoms

Once we have the learned dictionary of  $\mathbf{Y}$ , and therefore its sparse representation, we proceed to calculate the frequency vector  $\mathbf{f}$  of the dictionary  $\mathbf{D}$ . The frequency  $f$  of a dictionary atom  $d_i$  is equal to the number of signals that it affects, which is given by Equation 2, as illustrates Figure 4.

$$f(A_i) = \sum_{p=1}^P g(\alpha_{i,p}) \quad \forall i = 1, 2, \dots, K \quad (2)$$

$$g(\alpha_{i,p}) = \begin{cases} 1, & \forall \alpha_{i,p} \neq 0 \\ 0, & otherwise \end{cases} \quad (3)$$

Figure 4. Frequency concept of a dictionary atom  
 Figura 4. Ilustración del concepto de frecuencia de los átomos del diccionario



Then, the frequency vector  $F$  of  $D$  is defined as  $F=(f(d_1), f(d_2), \dots, f(d_k))$ . In Figure 4 the colored rectangles to the left represent the signals (linearized image patches) in  $Y$ , and the colored rectangles to the right represent the atoms in  $D$ . The arrows are non-zero values in  $\alpha$  which indicate what atoms  $d_i$  are linearly combined to approximate a signal  $y_i$ . Blue and black arrows point out signals affected (composed) by high-frequency atoms. On the other hand, red and green arrows point out signals affected by low-frequency atoms.

#### 5.4 Saliency map

After calculating the frequency of all the dictionary atoms, the saliency score of each signal is calculated to conform the saliency map of the image. The saliency score indicates whether the signal is composed of low-frequency atoms or not. If a signal is composed of low-frequency atoms, its score will be low and therefore must be classified as non-salient. The patch will be salient (rare signal) if it has a high score. Formally, the saliency score  $S$  of a signal  $y_i$  is given by Equation 4.

$$S(y_i) = \langle F, \alpha_i \rangle \quad (4)$$

Where  $\langle \cdot \rangle$  is the dot product and  $\alpha_i$  is the  $i$ -th column vector of  $\alpha$ , which is the sparse representation of  $y_i$  in  $D$ . The function of equation 4 is to accumulate the frequency of the atoms that compose  $y_i$ , but weighted by its associated factors in  $\alpha_i$ , i.e. it accumulates the frequency percentage (associated factor in  $\alpha_i$ ) of each atom that composes  $y_i$ . To obtain the saliency map  $S_{MAP}$  of  $I$ , we create first the saliency column matrix  $SCM$  (see Figure 5) of vectors  $S_i \in \mathbb{R}^{n \times 1}$ , where  $S_i = (S(i), S(i), \dots, S(i))^T$ .

Figure 5. Example of the SCM matrix. This matrix is made up of  $n$ -dimensional column vectors containing the saliency score of each signal in  $Y$

Figura 5. Ejemplo de la matriz SCM. Esta matriz se compone de vectores columna  $n$ -dimensionales los cuales contienen el puntaje de prominencia de cada señal de  $Y$

$$SCM = \begin{bmatrix} S(1) & S(2) & \dots & S(P) \\ S(1) & S(2) & \dots & S(P) \\ S(1) & S(2) & \dots & S(P) \\ \vdots & \vdots & \ddots & \vdots \\ S(1) & S(2) & \dots & S(P) \end{bmatrix}_{n \times P}$$

Then, the saliency map  $S_{MAP}$  of  $I$  is constructed from the  $SCM$  by converting each column into an image patch of  $\sqrt{n} \times \sqrt{n}$  and adding the overlapping cells. To both increase the saliency score of the salient regions, and decrease the score of non-salient ones, to achieve a better separation of these regions, the transform function, given by Equation 5, is applied to the  $S_{MAP}$ . In T1w axial brain MRI, structures like the ventricles look hypointense, and present low-frequency accumulation, as a result, look non-salient and therefore could be discarded. We use the convolution matrix  $ConvM$ , resulting from the application of Equation 7, for increasing the saliency score of the inner pixels of the axial brain MRI, to avoid discard such regions. Figure 6 shows two axial brain MRI T1 and T2 weighted with its corresponding  $S_{MAP}$ .

$$f(x) = 1 - e^{-x^2} \quad (5)$$

In this function, for big values of  $x$ ,  $f(x)$  is close to 1, and for small values of  $x$ ,  $f(x)$  is close to 0.  $x$  represents the saliency score of the corresponding pixel in the axial brain MRI.

$$ConvM_{i,j} = \beta e^{-\frac{d_{i,j}^2}{\beta}} \quad (6)$$

$$d_{i,j}^2 = \left(\frac{i-cr}{cr}\right)^2 + \left(\frac{j-cc}{cc}\right)^2 \quad (7)$$

where  $i$  and  $j$  are the index of row and column of  $ConvM$  respectively,  $\beta$  is a constant for controlling the dispersion of the Gaussian function,  $cr$  and  $cc$  are the index of the middle row and middle column respectively. Finally,  $S_{MAP} = ConvM \odot S_{MAP}$ . The operator  $\odot$  represents a bit-wise operation.

Figure 6.  $S_{MAP}$  of an axial brain MRI.  
 Figura 6.  $S_{MAP}$  de un corte axial de una IRM

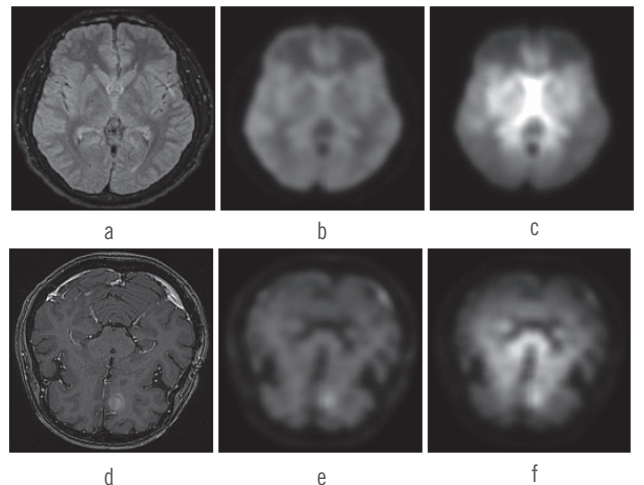


Figure 6a corresponds to an Axial T2 weighted brain MRI. Figure 6b is the  $S_{MAP}$  of Figure 6a after applying Equation 5. Figure 6c is the  $S_{MAP}$  after applying Equation 6 to Figure 6b. Figure 6d corresponds to an Axial T1 weighted brain MRI, Figure 6e is the  $S_{MAP}$  of figure 6d after applying Equation 5, and Figure 6f is the  $S_{MAP}$  after applying Equation 6 to Figure 6e. In figures, 6b and 6e can be observed how the saliency score of the brain tissue is higher than the score of the non-brain tissue. In Figures 6c and 6f, it is observed how was increased the saliency score of the inner pixels while the score of the outer ones was decreased after applying Equation 6.

### 5.5 Skull Stripping

Once we have the final  $S_{MAP}$  of  $I$ , we proceed to create the binary mask for eliminating the non-brain tissue. The mask is the result of applying Equation 8 to the  $S_{MAP}$  of  $I$ .

$$MK_{i,j} = \begin{cases} 1, & \text{if } S_{MAP_{i,j}} \geq T \\ 0, & \text{otherwise} \end{cases} \quad (8)$$

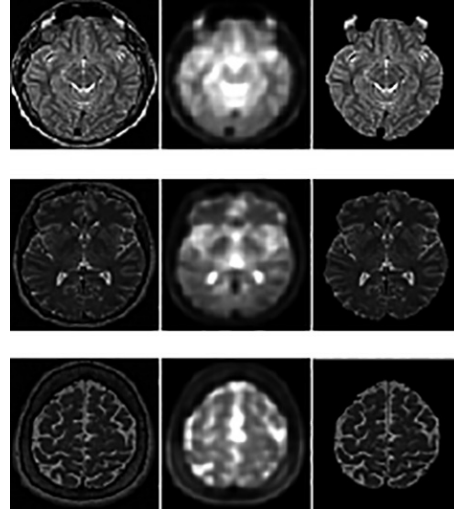
$T$  is a threshold value calculated as the mean of the pixels in  $S_{MAP}$ . After computing  $MK$ , the non-brain tissue is removed by operating  $I$  with  $MK$  through the bitwise operation  $I = MK \odot I$ .

As was mentioned before, in the deeper slices, the variety of patterns may result in salient regions corresponding to non-brain tissues, causing under-segmentation. And slices near to the top, may not have brain tissue. Therefore, for these slices, the process is propagated through a region growing algorithm, regarding the mean and the dispersion of the pixels corresponding to brain tissues in the middle slices. i.e. we compute the mean and the standard deviation from the neighbors pixels, corresponding to brain tissue, between the middle slices; then, through a region growing algorithm we propagate the skull stripping process to the remaining slices as follow: a pixel  $P_{i,j}$  belongs to brain tissue if it is neighbor of a brain tissue pixel in the previous slice and  $\mu - \sigma \leq P_{i,j} \leq \mu + \sigma$ , where  $\mu$  represents the mean value of the neighbors pixels in the previous slices, and  $\sigma$  its standard deviation.

## 6. RESULTS AND DISCUSSION

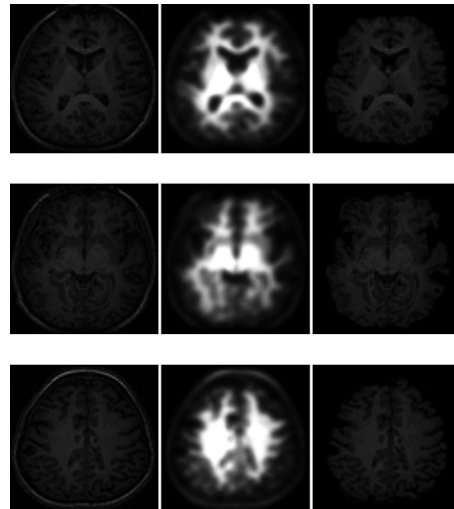
The proposed method for Skull Stripping of Brain MRI based on Saliency Detection (SSBSD) was testing using T1 and T2 weighted MRI. The processing was done in a Windows 10 64-bit OS workstation. A total of 50 T1w MRI were selected from Oxford, PaloAlto and Pittsburgh Data sets, of the ‘‘Child Mind Institute & International Neuroimaging Data-Sharing Initiative (INDI)’’ public database [29], and 20 T2w MRI were selected from ‘‘Designed Database of MR Brain Images of Healthy Volunteers’’ public database of MIDAS [30]. Figure 7 shows the result of the SSBSD applied on T2 weighted MRI.

Figure 7. Results of the SSBSD on T2 weighted MRIs. Figura 7. Resultados del SSBSD en IRMs ponderadas en T2



In Figure 7, the first column presents three slices of T2w axial brain MRIs. The images in the middle column represent the corresponding  $S_{MAP}$  of the images in the first column, and the images on the right column, correspond to the skull stripped images of the first column. It can be appreciated that the SSBSD method separates the cranial and fatty tissue without over-segmenting the image. The first axial brain MRI in Figure 7 presents under segmentation due to the outlier grey value of the non-brain tissue. Figure 8 shows the result of applying SSBSD on T1 weighted MRI. Our method has a good performance operating over T1w MRI, however, due to the low contrast of the images in Figure 8, a small over-segmentation was carried out. This can be observed in the second MRI (row two). In the first and the third MRI, almost no over-segmentation was carried out.

Figure 8. Results of the SSBSD on T1w MRI. Figura 8. Resultados del SSBSD en IRMs ponderadas en T1



In Figure 9 the SSBSD is compared to the BET [31], BSE [32], ROBEX [33] and S3 [16] methods. The ROBEX and the BSE are prone to sub-segmentation. In row two, there is a bit of over-segmentation in the BET and sub-segmentation in the S3 and the ROBEX, as indicated by the red circles. Table 1 summarizes the statistical results of the tests performed. The comparison is made with the DICE metric, given by Equation 9.

$$D(A, B) = \frac{2TP}{(FP + TP) + (FN + TP)} \quad (9)$$

Where *TP* are the true positives (pixels correctly classified as brain tissue), *FP* are the false positives (pixels incorrectly classified as brain tissue) and *FN* are the false negatives (brain tissue pixels classified as non-brain pixels).

Table 1. Summary of the tests performed  
Tabla 1. Resumen de las pruebas realizadas

Method	DICE	
	$\mu$	$\sigma$
BET	0.9789	0.0066
BSE	0.9603	0.0341
ROBEX	0.9732	0.0197
S3	0.9832	0.0057
SSBSD	0.9914	0.0051

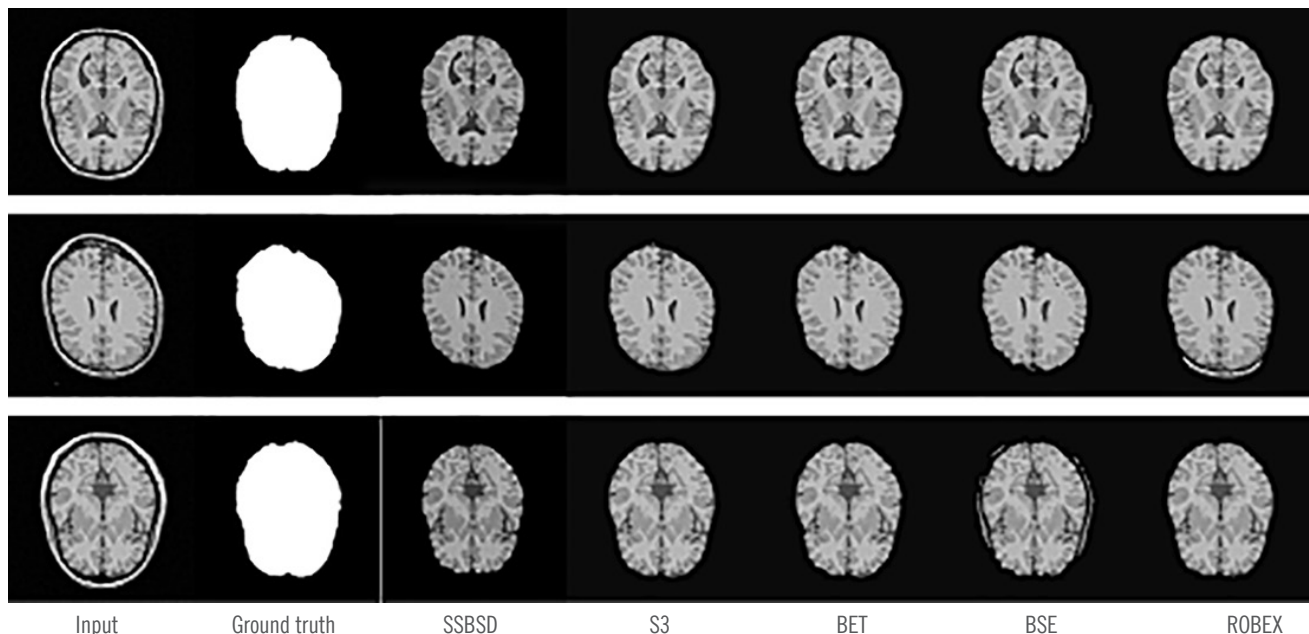
## 7. CONCLUSIONS AND FUTURE WORK

In this paper, a new approach for skull stripping based on saliency detection using dictionary learning was presented. Visual results show the effectiveness of the proposed method. It was demonstrated how the concept of saliency can be used for classifying brain tissue and non-brain tissue on axial brain MRI to carry out the skull stripping process. It was also shown, how detecting saliency on axial brain MRI by analyzing the sparse representation of the image. Our method can deal with T1 and T2 weighted MRI because it does not depend on the gray level of the image, but in the saliency of this. As future work, we will analyze how to estimate the more suitable threshold for avoiding the under and over-segmentation, mainly in T2 weighted MRI.

## ACKNOWLEDGMENTS

This research is partially supported by the Administrative Department of Science and technology of Colombia – COLCIENCIAS, under the program of doctoral scholarship COLCIENCIAS-UNINORTE 2015-006.

Figure 9. Comparison of the proposed method with S3, BET, BSE and ROBEX methods, applied on a T1w MRI  
Figura 9. Comparación del método propuesto con los métodos S3, BET, BSE y ROBEX, aplicados sobre una IRM ponderada en T1



## REFERENCES

- [1] J. V. Manjón, "Segmentación Robusta de Imágenes de RM cerebral," Universidad Politécnica de Valencia, Valencia - España, 2006.
- [2] P. Kalavathi and V. Surya Prasath, "Methods on Skull Stripping of MRI Head Scan Images—a Review," *Journal of Digital Imaging*, vol. 29, no. 3, p. 365–379, 2016.
- [3] C. Cecere, C. Corrado and R. Polikar, "Diagnostic Utility of EEG Based Biomarkers for Alzheimer's Disease," in *Annual Northeast Bioengineering Conference (NEBEC)*, Boston, USA, 2014.
- [4] B. S. Mahanand, S. Babu and S. Suresh, "Identification of imaging biomarkers responsible for Alzheimer's Disease using a McRBFN classifier," in *International Conference on Cognitive Computing and Information Processing (CCIP)*, Noida, India, 2015.
- [5] K. Dillon, C. Vince and Y.-P. Wang, "A robust sparse-modeling framework for estimating schizophrenia biomarkers from fMRI," *Journal of Neuroscience Methods*, vol. 276, pp. 46-55, 2017.
- [6] E. M. Meisenzahl, N. Koutsouleris, R. Bottlender, J. J. M. Scheurecker, S. J. Teipel, S. Holzinger, T. Frodl, U. Preuss, G. Schmitt, B. Burgermeister, M. Reiser, C. Born and H. J. Möller, "Structural brain alterations at different stages of schizophrenia: A voxel-based morphometric study," *Schizophrenia Research*, vol. 104, no. 1-3, pp. 44-60, 2008.
- [7] E. H. Aylward, "Change in MRI striatal volumes as a biomarker in preclinical Huntington's disease," *Brain Research Bulletin*, vol. 72, p. 152–158, 2007.
- [8] A. Plerou, C. Bobori and P. Vlamos, "Molecular Basis of Huntington's Disease and Brain Imaging Evidence," in *IEEE International Symposium on Signal Processing and Information Technology (ISSPIT)*, Abu Dhabi, UAE, 2015.
- [9] L. Wang, Y. Chen, X. Pan, X. Hong and D. O Xia, "Level set segmentation of brain magnetic resonance images based on local gaussian distribution fitting energy," *Journal of Neuroscience Methods*, vol. 188, no. 2, p. 316–325, 2010.
- [10] S. Roy and P. Maji, "An accurate and robust skull stripping method for 3-D magnetic resonance brain images," *Magnetic Resonance Imaging*, vol. 54, pp. 46-57, 2018.
- [11] S. Roy, J. A. Butman and D. L. Pham, "Robust skull stripping using multiple MR image contrasts insensitive to pathology," *NeuroImage*, vol. 146, no. 1, pp. 132-147, 2017.
- [12] J. Kleesiek, G. Urban, A. Hubert, D. Schwarz, K. Maier-Hein, M. Bendszus and A. Biller, "Deep MRI brain extraction: A 3D convolutional neural network for skull stripping," *NeuroImage*, vol. 129, no. 1, pp. 460-469, 2016.
- [13] R. Shaswati and M. Pradipta, "A simple skull stripping algorithm for brain MRI," in *Eighth International Conference on Advances in Pattern Recognition (ICAPR)*, Kolkata, India, 2015.
- [14] K. Somasundaram and P. Kalavathi, "Contour-based brain segmentation method for magnetic resonance imaging human head scans," *Journal of Computer Assisted Tomography*, vol. 37, no. 3, p. 353–368, 2013.
- [15] M. Brummer, R. Mersereau, R. Eisner and R. Lewine, "Automatic detection of brain contours in MRI data sets," *IEEE Transactions on Medical Imaging*, vol. 12, no. 2, pp. 153-166, 1993.
- [16] S. Roy and P. Maji, "A Simple Skull Stripping Algorithm for Brain MRI," in *Eighth International Conference on Advances in Pattern Recognition (ICAPR)*, Kolkata, India, 2015.
- [17] J. Kleesiek, G. Urban, A. Hubert, D. Schwarz, K. Maier-Hein, M. Bendszus and A. Biller, "Deep MRI Brain Extraction: A 3D Convolutional Neural Network for Skull Stripping," *NeuroImage*, vol. 129, no. 1, pp. 460-469, 2016.
- [18] S. Goferman, L. Zelnik-Manor and A. Tal, "Context-Aware Saliency Detection," *IEEE Transactions on Pattern Analysis and Machine Intelligence*, vol. 34, no. 10, pp. 1915 - 1926, 2012.
- [19] K. Guo and H.-T. Chen, "Learning sparse dictionaries for saliency detection," in *Signal & Information Processing Association Annual Summit and Conference (APSIPA ASC)*, Hollywood, CA, USA, 2012.
- [20] N. Li, B. Sun and J. Yu, "A weighted sparse coding framework for saliency detection," in *IEEE Conference on Computer Vision and Pattern Recognition (CVPR)*, Boston, MA, USA, 2015.
- [21] J. Yang and M.-H. Yang, "Top-Down Visual Saliency via Joint CRF and Dictionary Learning," *IEEE Transactions on Pattern Analysis and Machine Intelligence*, vol. 39, no. 3, p. 576–588, 2017.
- [22] R. Cong, J. Lei, H. Fu, M.-M. Cheng, W. Lin and Q. Huang, "Review of Visual Saliency Detection with Comprehensive Information," *IEEE TRANSACTIONS ON CIRCUITS AND SYSTEMS FOR VIDEO TECHNOLOGY*, pp. 1-19, 2018.
- [23] W. Zhu, S. Liang, W. Yichen and J. Sun, "Saliency Optimization from Robust Background Detection," Columbus, OH, USA, 2014.
- [24] I. Rish, "Functional MRI Analysis with Sparse Models," in *Joint European Conference on Machine Learning and Knowledge Discovery in Databases - ECML PKDD 2013*, Prague, 2013.
- [25] M. Liu, D. Zhang, D. Shen and T. A. D. N. Initiative, "Ensemble sparse classification of Alzheimer's disease," *NeuroImage*, vol. 60, pp. 1106-1116, 2012.
- [26] C. Bao and H. Ji, "Dictionary Learning for Sparse Coding: Algorithms and Convergence Analysis," *IEEE Transactions on Pattern Analysis and Machine Intelligence*, vol. 38, no. 7, pp. 1356 - 1369, 2016.
- [27] M. Aharon, M. Elad and A. M. Bruckstein, "The K-SVD: an algorithm for designing of overcomplete dictionaries for sparse representation," *IEEE Transactions On Signal Processing*, vol. 54, no. 11, pp. 4311-4322, 2006.
- [28] M. Aharon, M. Elad and A. M. Bruckstein, "On the uniqueness of overcomplete dictionaries, and a practical way to retrieve them," *Journal of Linear Algebra and Applications*, vol. 416, pp. 48-67, 2006.
- [29] C. M. Institute and I. N. D.-S. I. (INDI), "1000 Functional Connectomes Project," Child Mind Institute & International Neuroimaging Data-Sharing Initiative (INDI), 2017. [Online]. Available: [http://feon\\_1000.projects.nitrc.org/](http://feon_1000.projects.nitrc.org/). [Accessed 20 8 2018].
- [30] MIDAS, "Designed Database of MR Brain Images of Healthy Volunteers," MIDAS, 2010. [Online]. Available: <http://insight-journal.org/midas/community/view/21>. [Accessed 7 10 2018].
- [31] S. M. Smith, "Fast robust automated brain extraction," *Human Brain Mapping*, vol. 17, no. 3, pp. 143-155, 2002.
- [32] D. W. Shattuck and R. M. Leahy, "BrainSuite: an automated cortical surface identification tool," *Medical Image Analysis*, vol. 6, no. 2, pp. 129-142, 2002.
- [33] J. E. Iglesias, C. Y. Liu and P. M. T. Z. Thompson, "Robust brain extraction across datasets and comparison with publicly available methods," *IEEE Transactions on Medical Imaging*, vol. 30, no. 9, pp. 1617-1634, 2011.